Analysis, predicting, and controlling the COVID-19 pandemic in Iraq through SIR model

Sanaa L. Khalaf *, Hadeer S. Flayyih

Department of Mathematics, College of Science, University of Basrah, Basrah, Iraq

ARTICLE INFO

ABSTRACT

Using the standard SIR model with three unknown biological parameters, the COVID-19 pandemic in Iraq has been studied. The least squares method and real data on confirmed infections, deaths, and recoveries over a long time (455 days) were used to estimate these parameters. In this regards, first, we find the basic reproductive number R_0 is 0.9422661124 which indicates and predicts that the COVID-19 pandemic in Iraq will gradually subside until it is eradicated permanently with time. Additionally, we develop an optimal vaccination strategy with the goal of reducing COVID-19 infections and preventing their spread in Iraq, thereby putting a clear picture of control this pandemic.

1. Introduction

Since its emergence over two years ago, the COVID-19 pandemic has overtaxed the ability of healthcare organizations throughout much of the world, affecting virtually every aspect of daily life. In fact, the last days of 2019 brought an unwelcome surprise: the first pandemic of the century. Wuhan, the capital of the Chinese province of Hubei, was the first place that COVID-19 appeared, and then it spread from Wuhan to around the world. This necessitated pooling all of the world's resources to combat the looming pandemic and halt its spread in any way possible, as most countries closed their borders and airports and prohibited citizens from roaming freely for fear of the disease spreading further. During this time, major pharmaceutical companies worldwide rushed to produce vaccines, and the FDA approved some vaccines for emergency use, including those manufactured by Pfizer, Moderna, and AstraZeneca [1].

In recent years, the mathematical modeling of infectious diseases has become an active and important area of research being carried out. Because infectious diseases have dynamic behaviors, mathematical epidemiology can help scientists to better understand how they behave and what they can expect in the future. In fact, mathematical models are usually implemented to compare and evaluate various detection, prevention, therapy, and control programs, as well as to plan, implement, evaluate, and optimize these programmers throughout their lifecycle. In this vein, many studies have been published in recent years that have been adopted for the creation and evaluation of epidemiological models, and many of these contain significant findings [2–4]. Since the new pandemic's emergence, a slew of mathematical models has given health officials in many countries some useful insights into the most effective ways to stop the disease from spreading [5–9].

Recently, the mathematical models provide future insight into the qualitative behavior of COVID-19 and give a prediction of how this disease will behave [5,10–15]. Some scholars in Ontario, Canada, offered a mathematical model to examine the impact of a variety of public interventions on COVID-19 behavior and how to reduce it [16]. Depending on nonlinear differential equations, Fanelli and Piazza have discussed the temporal models for COVID-19 infection in three countries: China, Italy, and France, based on the real dates of certain days [17]. While Khan and Atangana used the COVID-19 confirmed infection reports in Wuhan to develop
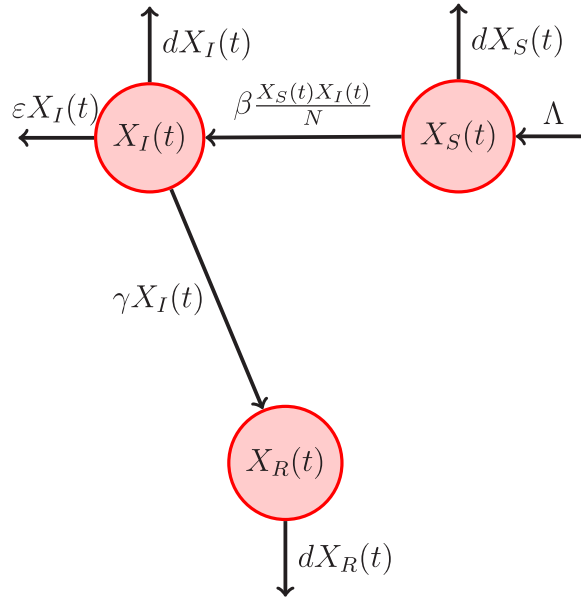
Fig. 1. SIR model flowchart.

and analyze a fractional model by using fractional derivatives [6]. In the absence of any available vaccine or treatment at that time, Atangana studied effects of curfew on population to mitigate the infection of COVID-19 [18]. Also, Sahin and Sahin introduced a fractional model depending on the cumulative daily report of COVID-19 in three countries: Italy, UK, and USA, to study the transmission of this disease [19]. In Mexico, some authors used artificial neural networks to perform and predict the transmission model of COVID-19 [20]. Also, Based on real data from Ghana, many models for COVID-19 have been investigated, as the reader can see in [21–24]. Some scholar investigate the impact of self-isolation, quarantine, and contact tracing on the stopping and control of the COVID-19 pandemic using data from the New York population [25]. On the other hand, fractional differential equations play a fundamental role in the distribution of the COVID-19 pandemic [26,27], so there are numerous methods to solve them [28–31].

In this study, we use the standard SIR to describe COVID-19 transmission in Iraq in order to help the Iraqi Ministry of Health develop a vaccination strategy. To begin, we used real data from confirmed infections over a period of 455 days to develop the model. After that, a sensitivity analysis is performed to see how parameters affect R_0. To reduce the number of infected people and develop an optimal vaccination strategy, we constructed a quadratic optimal control problem. We hope that the strategy outlined in this paper will help predict the long-term trend of COVID-19 and reduce the number of infected people.

2. The SIR model and parameters fitting results

Now, the following standard SIR model will be use to study COVID-19 pandemic in Iraq.

$$\begin{aligned}
\frac{dX_S}{dt} &= \Lambda - \frac{\beta X_I(t) X_S(t)}{(X_S(t) + X_I(t) + X_R(t))} - dX_S(t), \\
\frac{dX_I}{dt} &= \frac{\beta X_I(t) X_S(t)}{(X_S(t) + X_I(t) + X_R(t))} - (\gamma + \epsilon + d)X_I(t), \\
\frac{dX_R}{dt} &= \gamma X_I(t) - dX_R(t),
\end{aligned} \tag{2.1}$$

where the biological parameters Λ, β, d, γ, and ϵ are represent the birth rate, the disease transmission rate, the natural death rate, the recovery rate, and the disease death rate respectively (see Fig. 1).

Now, we adopt the use of model parameter estimation to examine the model's validity and reliability by comparing and fitting the SIR model with actual data. This will show the accuracy and the ability of the considered model to predict real results. The country of Iraq will be used as an example in this section. Also, the daily reports of COVID-19 by the WHO and the Iraqi Ministry of Health will be considered for this purpose. To give a complete picture of this subject, we collected data on cases of confirmed infection, death, and recovery for a long period of 455 days starting from January 1, 2021, to March 31, 2022.

According to Iraq demographics reported by U.N. [32] the life expectancy at birth of Iraqi people, both sexes, is 71.08 year, and the estimated number of population of Iraqi people is approximately N(0)= 41828817. Therefore the natural death rate parameter d and the birth rate Λ of Iraqi population in the disease absence are $d = 1/(71.08 \times 365)$ per day and $\Lambda = d \times N(0) = 1635$ per day.

It is well known that the key to designing any epidemiological study is to figure out how many biological parameters to use in it and how to estimate them. In fact, in this study, we try to implement the stander SIR model with three unknown parameters to
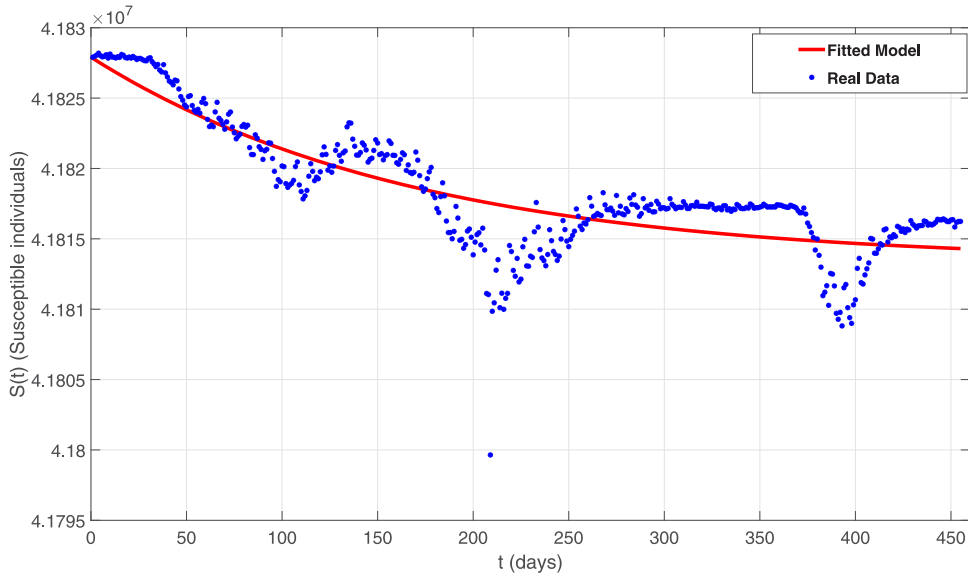
Fig. 2. Fitted diagram of susceptible individuals in Iraq and the SIR model.

study the behavior of COVID-19 pandemic in Iraq. Thus, the main effort of this work is to focus on how to estimate these parameters to ensure the validity of the suggested SIR model. For this purpose, the least squares method will be used.

As a practical matter, we will use days as the time unit, and the observed collected data on the confirmed infected cases $\tilde{I}$, death cases $\tilde{D}$, and recovered cases $\tilde{R}$ for a long period of 455 days. The first step is to use these observed collected data to compute the number of susceptible people according to the following relationship:

$$\tilde{X}_S(t) = N(t) - \tilde{X}_I(t) - \tilde{X}_R(t) - dN(t), \quad t = 0, 1, 2, \ldots, \tag{2.2}$$

where $N(t)$ is defined by

$$N(t) = (1-d)N(t-1) + \Lambda, \quad t = 1, 2, 3, \ldots \tag{2.3}$$

Now, we are ready to apply the least squares method to estimate the value of β, γ and ϵ. Therefore, we will construct the objective function, which is the sum of square errors, as follows:

$$E(\beta, \gamma, \epsilon) = \sum_{\kappa=0}^{M} (X_S(\kappa) - \tilde{X}_{S_\kappa})^2 + (X_I(\kappa) - \tilde{X}_{I_\kappa})^2 + (X_R(\kappa) - \tilde{X}_{R_\kappa})^2, \tag{2.4}$$

where M is the total number of days with available observed data in our study, which is 455. Also, $X_S(\kappa), X_I(\kappa)$, and $X_R(\kappa)$ are the estimated values at the day κ, which satisfied the Eq. (2.1). In order to determine the unknown biological parameters, we must first solve the optimization problems listed below:

$$Minimize \ E(\beta, \gamma, \epsilon) \tag{2.5}$$
$$S.T. \qquad Eq.(2.1)$$

In fact, we will use two Matlab packages, ode45 (Runge–Kutta methods) and lsqcurvefit (least-square curve fitting), to perform the above task. The optimal fit to available collected data of susceptible individuals via $X_S(t)$ of our SIR model is illustrated in Fig. 2 and the corresponding estimated parameters are $\beta = 0.0953$, $\gamma = 0.0162$, and $\epsilon = 0.0849$.

3. Stability analysis of the SIR model

In order to make predictions and have a clear image about the future behavior of the Covid-19 pandemic in Iraq, we will focus in this section on studying the behavior of the model (2.1) near the equilibrium points as time increases. First, we solve the next equations

$$\Lambda - \frac{\beta X_I X_S}{(X_S + X_I + X_R)} - dX_S = 0,$$
$$\frac{\beta X_I X_S}{(X_S + X_I + X_R)} - (\gamma + \epsilon + d)X_I = 0, \tag{3.1}$$
$$\gamma X_I - dX_R = 0.$$

Now, we can deduce that the model (2.1) possesses two equilibrium points as follows:

1. The equilibrium point free of disease E_0 which given by:

$$E_0 = (X_{S_0}, X_{I_0}, X_{R_0}) = (\frac{\Lambda}{d}, 0, 0). \tag{3.2}$$

2. The endemic equilibrium point E_e which given by:

$$E_e = (X_{S_e}, X_{I_e}, X_{R_e}) = (\frac{\Lambda - (\gamma + d + \varepsilon)X_I}{d}, X_I, \frac{\gamma X_I}{d}). \tag{3.3}$$

Here we emphasize that the compounds of point E_0 are free of X_I, unlike the compounds of point E_e that contain X_I which they were named.

3.1. The basic reproductive number R_0

In this subsection, we will look into the vital threshold and chief quantity, well-known as the basic reproduction number, which is commonly abbreviated as R_0. In fact, R_0 performs a critical function in the disease-free local stability as documented by [33].

Now, calculate R_0, where R_0 is the eigenvalue of the matrix $G = FV^{-1}$, where F indicates new infections, while V indicates the transmission of infection from one place to another. Both are calculated in an equilibrium-free equilibrium state and are thus derived as follows.

Infectious compartments are found in the system (2.1) as follows.

$$\frac{dX_S}{dt} = \Lambda - \frac{\beta X_I(t)X_S(t)}{(X_S(t) + X_I(t) + X_R(t))} - dX_S(t),$$
$$\frac{dX_I}{dt} = \frac{\beta X_I(t)X_S(t)}{(X_S(t) + X_I(t) + X_R(t))} - (\gamma + \varepsilon + d)X_I(t). \tag{3.4}$$

Let $\Omega = [X_I, X_S]^T$. Then the system (3.4) can be written as

$$^C_0 D^\alpha_t \Omega = \tilde{F}(\Omega) - \tilde{V}(\Omega), \tag{3.5}$$

where

$$\tilde{F}(\Omega) = \begin{bmatrix} \frac{\beta X_I(t)X_S(t)}{(X_S(t) + X_I(t) + X_R(t))} \\ 0 \end{bmatrix}, \tag{3.6}$$

and

$$\tilde{V}(\Omega) = \begin{bmatrix} (\gamma + \varepsilon + d)X_I(t) \\ -\Lambda + \frac{\beta X_I(t)X_S(t)}{(X_S(t) + X_I(t) + X_R(t))} + dX_S(t) \end{bmatrix}, \tag{3.7}$$

Therefore, we perform the calculation of the matrices F and V at the point E_0 in the following forms:

$$F = \begin{bmatrix} 0 & \beta \\ 0 & 0 \end{bmatrix}, \tag{3.8}$$

and

$$V = \begin{bmatrix} 0 & \gamma + d + \epsilon \\ d & \beta \end{bmatrix}, \tag{3.9}$$

Matrix V is inversed as follows

$$V^{-1} = \begin{bmatrix} -\frac{\beta}{(\gamma + d + \epsilon)d} & \frac{1}{d} \\ \frac{1}{\gamma + d + \epsilon} & 0 \end{bmatrix}. \tag{3.10}$$

Now, by multiplying matrices (3.8) and (3.10) we will get

$$G = \begin{bmatrix} \frac{\beta}{\gamma + d + \epsilon} & 0 \\ 0 & 0 \end{bmatrix}. \tag{3.11}$$

Since, the eigenvalues of the matrix (3.11) are $\lambda_1 = 0$, and $\lambda_2 = \frac{\beta}{\gamma + d + \epsilon}$, we have

$$R_0 = \frac{\beta}{\gamma + d + \epsilon}. \tag{3.12}$$

It is important to note that when R_0 less than one, disease in the population is eradicated and infection is eliminated. Furthermore, when R_0 is greater than one, the disease will continue to exist in the population. Therefore, based on the estimated COVID-19 pandemic parameters in Iraq for the available time period starting from January 1, 2021, to March 31, 2022, we find that $R_0 = 0.9422661124$, indicating that the COVID-19 pandemic in Iraq will gradually reduce until it is permanently ended with the passage of time.

Table 1
Table of sensitivity indices.

Symbol for a parameter	Indexes of sensitivity
β,	+ve
γ	−ve
ϵ	−ve

3.2. A sensitivity analysis of R_0

Due to the fact that R_0 is an extremely biologically significant quantity that plays a chief role in the spread of any pandemic, investigating the sensitivity of R_0 is very interesting and crucial to the elimination and effective control of the disease. R_0 sensitivity to changes in parameter Y is represented by this index. So, we can calculate the changes in all parameters in the formula of R_0 by using the partial derivatives as follows:

Now, we give the following relationship that describes the R_0 forward sensitivity index with respect to the parameter Y:

$$\Theta_Y^{R_0} = \left(\frac{\partial R_0}{\partial Y} \right) \left(\frac{Y}{R_0} \right), \tag{3.13}$$

where Y is a parameter to describe the basic reproductive number R_0. It is well known that a negative (positive) index means that any increase in the parameter Y leads to a decrease (increase) in R_0 [34]. The sensitivity indices with respect to the parameters can be given β, ϵ, and γ respectively, by the basic reproductive number mentioned in the Eq. (3.12), as follows:

$$\frac{\partial R_0}{\partial \beta} \frac{\beta}{R_0} = \frac{1}{\gamma + d + \epsilon} \frac{\beta}{R_0},$$
$$= \frac{1}{\gamma + d + \epsilon} \frac{\beta}{\frac{\beta}{\gamma + d + \epsilon}} = 1.$$

$$\frac{\partial R_0}{\partial \epsilon} \frac{\epsilon}{R_0} = \frac{-\beta}{(\gamma + d + \epsilon)^2} \frac{\epsilon}{\frac{\beta}{\gamma + d + \epsilon}},$$
$$= \frac{-\epsilon}{\gamma + d + \epsilon} = -0.8394374916.$$

$$\frac{\partial R_0}{\partial \gamma} \frac{\gamma}{R_0} = \frac{-\beta}{(\gamma + d + \epsilon)^2} \frac{\gamma}{\frac{\beta}{\gamma + d + \epsilon}},$$
$$= \frac{-\gamma}{\gamma + d + \epsilon} = -0.1601753518.$$

In fact, Table 1 describes and explains the R_0 sensitivity indices to biological parameters for the considered model, as determined using the estimated parameter values computed in Section 2, where the parameters are listed in decreasing order of sensitivity. The result demonstrated that when the disease transmission rate parameter is increased while the other parameters are kept fixed, the value of R_0 is increased, which means that we will experience an endemicity of the disease more since it has positive indices. On the other hand, the increase of the parameters γ, and ϵ will lead to a decrease in the value of R_0 which means that we will probably reduce the chance of spreading the disease more since these parameters have negative indices.

4. Optimal control on the model

In order to design an optimal vaccination strategy to minimize the number of COVID-19 infections and prevent its spread in Iraq, we reformulate the SIR model in Eq. (2.1) by imposing a control variable that represents the effect of the vaccine. Also, we will take into consideration the number of days, $\tau = 14$ days, that the vaccine will start working actively as in Fig. 3 and the following time-delay differential equations:

$$\frac{dX_S}{dt} = \Lambda - \frac{\beta X_I(t) X_S(t)}{(X_S(t) + X_I(t) + X_R(t))} - dX_S(t) - u(t - \tau) X_S(t - \tau),$$
$$\frac{dX_I}{dt} = \frac{\beta X_I(t) X_S(t)}{(X_S(t) + X_I(t) + X_R(t))} - (\gamma + \epsilon + d) X_I(t), \tag{4.1}$$
$$\frac{dX_R}{dt} = \gamma X_I(t) - dX_R(t) + u(t - \tau) X_S(t - \tau).$$

In addition, the cost function is constructed as follows:

$$\mathfrak{I}(u(t)) = \int_0^{t_f} \left(D_1 X_I(t) + \frac{D_2}{2} u^2(t) \right) dt, \tag{4.2}$$

where D_1 and D_2 are the balancing cost factors and t_f is the specific time. From this point on, our primary goal is to optimally figure out the most effective vaccination controls so that we can limit the speed of the spread of this epidemic, reduce mortality, and
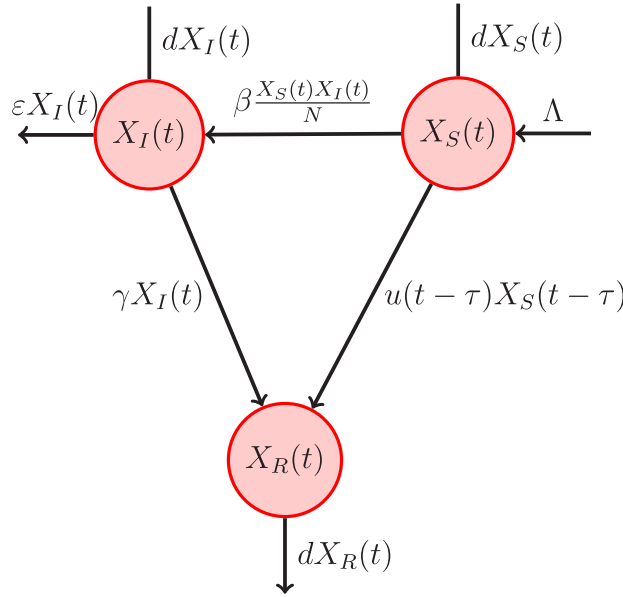
Fig. 3. Time delay SIR model flowchart.

avoid unnecessary complications. As a result, our task will be to find the control variable $u(t)$ between zero and one that minimizes $\mathfrak{I}(u(t))$ under the constraints of Eq. (4.1).

In other words, we want to find the optimal vaccination controls, $u^*(t)$ that satisfied:

$$\mathfrak{I}(u^*(t)) = min\{\mathfrak{I}(u(t)) : 0 \leq u(t) \leq 1, \forall t \in [0, t_f] \text{ such that the state equations are satisfied}\}.$$

Therefore, we will use the minimum principle of Pontryagin, which is modified in [35], to find the optimal control solution for our problem that have delays in control and state variables.

For this purpose, we define the following Hamiltonian function:

$$H = D_1 X_I(t) + \frac{D_2}{2}u^2(t) + \sum_{\kappa=1}^{3} p_1(t)f_\kappa(X_S(t), X_I(t), X_R(t), U(t-\tau), X_S(t-\tau)), \tag{4.3}$$

where f_κ denotes the right side of the κth equation's SIR model.

Now, according the minimum principle of Pontryagin in [35], we have the optimal control $u^*(t)$ by

$$u^*(t) = max\{0, min\{1, \frac{p_1^+(t) - p_2^+(t)}{D_2} \hbar_{[0, t_f - \tau]}(t) X_S^*(t)\}\}, \quad \forall t \in [0, t_f], \tag{4.4}$$

where

$$\hbar_{[0, T_f - \tau]}(t) = \begin{cases} 1, & t \in [0, t_f - \tau] \\ 0, & otherwise \end{cases}. \tag{4.5}$$

Also, the co-state variables $p_1(t), p_2(t)$ and $p_3(t)$ at the optimal solution $X_S^*(t), X_I^*(t), X_R^*(t)$ and $u^*(t)$ satisfy the following differential equations:

$$\frac{dp_1(t)}{dt} = d\,p_1(t) + \frac{\beta(p_1(t) - p_2(t))}{N^*(t)}X_I^*(t) + \hbar_{[0, t_f - \tau]}(t)(p_1(t) - p_3(t))u^*(t),$$

$$\frac{dp_2(t)}{dt} = -D_1 + \frac{\beta(p_1(t) - p_2(t))}{N^*(t)}X_S^*(t) + (\varepsilon + d + \gamma)p_2(t) - \gamma p_3(t), \tag{4.6}$$

$$\frac{dp_2(t)}{dt} = \gamma p_3(t),$$

with terminal transversality conditions, $p_1(t_f) = 0, p_2(t_f) = 0,$ and $p_3(t_f) = 0$. Also, $p_\kappa^+(t) = p_\kappa(t + \tau),$ for $\kappa = 1, 2, 3$.

To find the optimal vaccination strategy, we construct the following algorithm based on applying the forward and backward Euler method to solve state Eq. (4.1) and co-state equations Eq. (4.6), respectively, and on the optimal control law in Eq. (4.4).

Algorithm 4.1.

Step 1 *Insert the values of the biological parameters $\Gamma, d, \beta, \gamma, \epsilon,$ and τ. Also, insert the initial conditions of $X_S(\kappa) = X_S(0), X_I(\kappa) = X_I(0), X_R(\kappa) = X_R(0)$ for all $\kappa = -M, -M+1, \ldots, 0$ and terminal conditions $p_1(\kappa), p_2(\kappa), p_3(\kappa) = 0,$ for all $\kappa = N, N+1, \ldots, N+M$.*
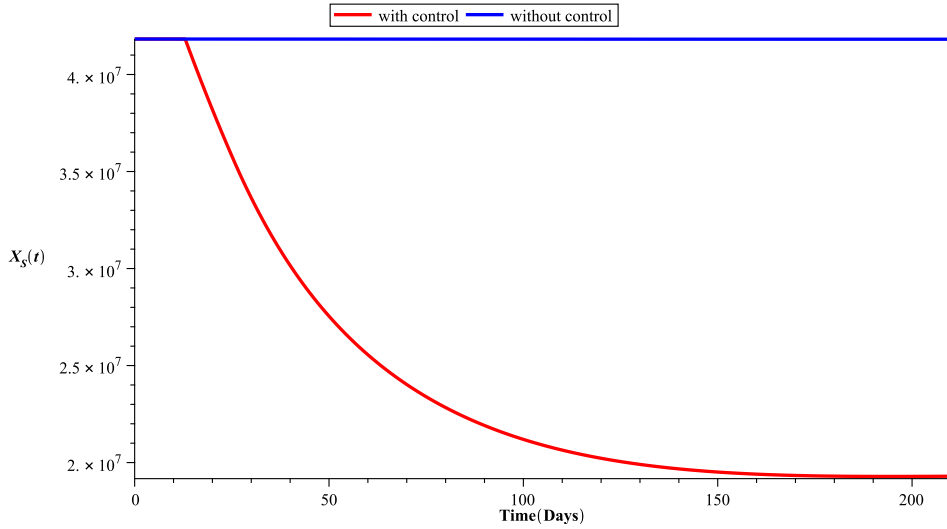
Fig. 4. The susceptible $X_S(t)$ without and with control. (For interpretation of the references to color in this figure legend, the reader is referred to the web version of this article.)

Step 2 *Suppose the time interval is $[0, t_f]$ and compute the step size $h = \frac{t_f}{N} = \frac{\tau}{M}$, where N and M are positive integer numbers.*

Step 3 *Set $u(\kappa h) = 0$, for all $\kappa = -M, -M+1, \ldots, 0, 1, \ldots, N$.*

Step 4 *For all $\kappa = 1, 2, \ldots, N$, compute $X_S(\kappa h), X_I(\kappa h)$, and $X_R(\kappa h)$ by applying forward Euler method as follows:*

$$X_S((\kappa+1)h) = X_S(\kappa h) + h(\Lambda - \frac{\beta X_I(\kappa h) X_S(kh)}{(X_S(\kappa h) + X_I(kh) + X_R(kh))} - d\, X_S(\kappa h)),$$

$$- u(h(\kappa - M)) X_S(h(\kappa - M))$$

$$X_I((\kappa+1)h) = X_I(\kappa h) + h(\frac{\beta X_I(\kappa h) X_S(\kappa h)}{(X_S(kh) + X_I(\kappa h) + X_R(\kappa h))} - (\gamma + \epsilon + d) X_I(\kappa h)),$$

$$X_R((\kappa+1)h) = X_R(\kappa h) + h(\gamma X_I(\kappa h) - d\, X_R(\kappa h)) + u(h(\kappa - M)) X_S(h(\kappa - M)).$$

Step 5 *For all $\kappa = N-1, N-2, \ldots, 0$, compute $p_1(\kappa h), p_2(\kappa h)$, and $p_3(\kappa h)$ by applying backward Euler method as follows:*

$$p_1(\kappa h) = p_1((\kappa+1)h) - h(d p_1((\kappa+1)h) + \frac{\beta(p_1((\kappa+1)h) - p_2((\kappa+1)h))}{(X_S((\kappa+1)h) + X_I((\kappa+1)h) + X_R((\kappa+1)h))}$$

$$\times X_I((\kappa+1)h) + \hbar_{[0,t_f - \tau]}((\kappa+1)h)(p_1((\kappa+1)h) - p_3((\kappa+1)h))u((\kappa+1)h)),$$

$$p_2(\kappa h) = p_2((\kappa+1)h) - h(-D_1 + \frac{\beta(p_1((\kappa+1)h) - p_2((\kappa+1)h))}{(X_S((\kappa+1)h) + X_I((\kappa+1)h) + X_R((\kappa+1)h))}$$

$$\times X_S((\kappa+1)h) + (\epsilon + d + \gamma)p_2((\kappa+1)h) - \gamma p_3((\kappa+1)h)),$$

$$p_2(\kappa h) = p_2((\kappa+1)h) - h\gamma p_3((\kappa+1)h).$$

Step 6 *Apply the optimal control law to compute $u(kh)$ for all $\kappa = 1, 2, \ldots, N$ as follows:*

$$u(\kappa h) = max\{0, min\{1, \frac{p_1(\kappa h + M) - p_2(\kappa h + M)}{D_2} \hbar_{[0,t_f - \tau]}(\kappa h) X_S^*(\kappa h)\}\}.$$

Step 7 *If the stopping criterion (the absolute value of optimal control of the current and the previous iterations) is held, then the algorithm ends, else return to Step 4.*

5. Numerical simulation of optimal vaccination strategy

This section focuses on introducing a numerical simulation of an optimal vaccination strategy by solving the optimal control problem that was constructed in the previous section. Indeed, the optimal control solution was calculated using the estimated parameters, the Algorithm 4.1, and Maple2020 software. The results appear to show the impact of the vaccination process in controlling and preventing the outbreak of this pandemic in Iraq. We show that if Iraq's healthcare system followed the vaccination process depicted in Fig. 7, the number of infected people would decrease as depicted in Fig. 6, while the number of vaccinated and recovered people would increase as depicted in Fig. 5.
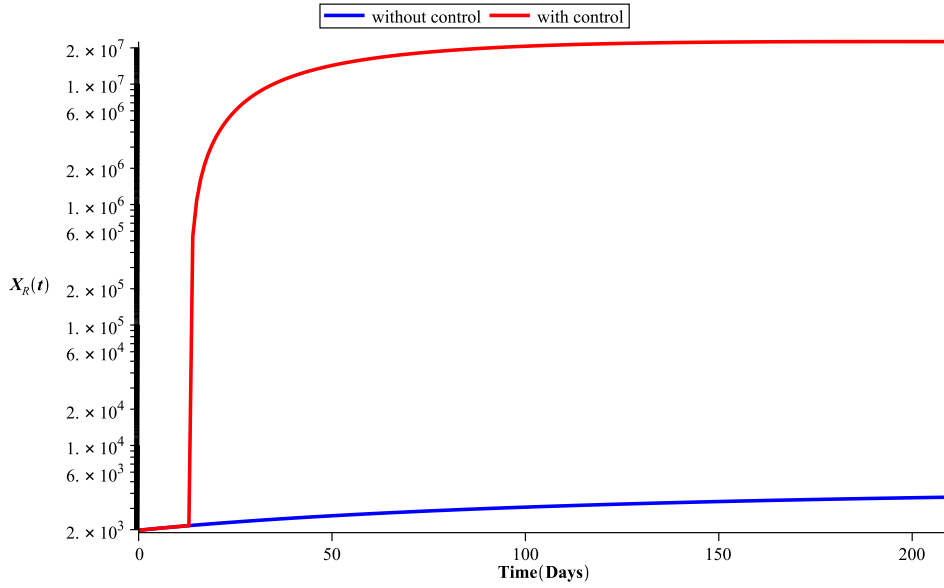
Fig. 5. The recovery $X_R(t)$ without and with control. (For interpretation of the references to color in this figure legend, the reader is referred to the web version of this article.)
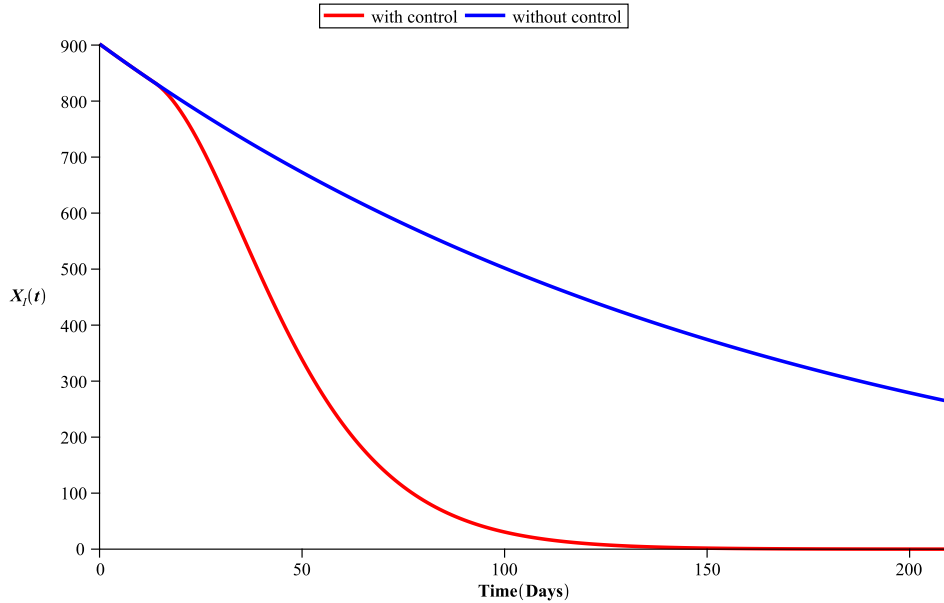
Fig. 6. The infections $X_I(t)$ without and with control. (For interpretation of the references to color in this figure legend, the reader is referred to the web version of this article.)

6. Conclusions

We use SIR model with three unknown parameters to study the behavior of COVID-19 pandemic in Iraq. In fact, there are two main parts of our work: The first is using the real data on cases of confirmed infection, death, and recovery for a long period of 455 days starting from January 1, 2021, to March 31, 2022 (see Appendix) to estimation these three unknown parameters as in Section 2. Also, we compute the basic reproductive number R_0 and study the sensitive analysis of each effective parameters. In fact, R_0 indicates and predicts that the COVID-19 pandemic in Iraq will gradually subside until it is eradicated permanently with time. The
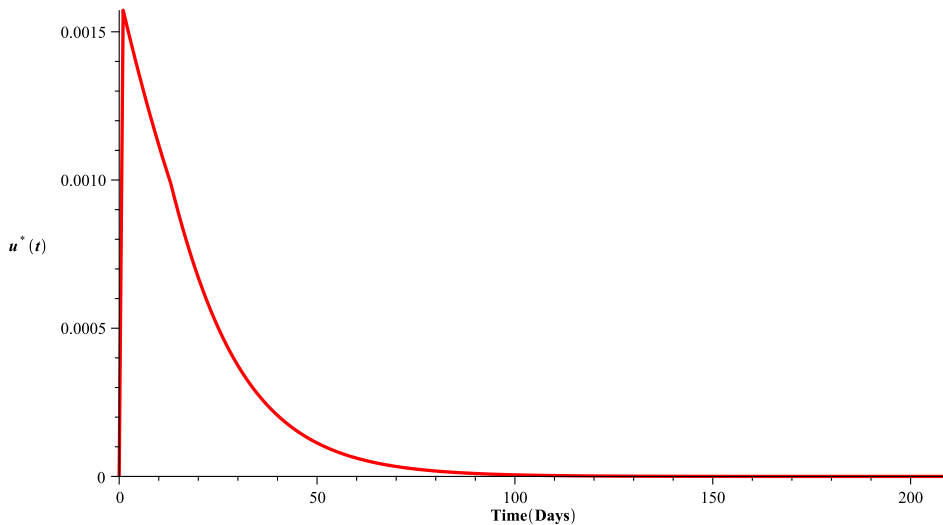
Fig. 7. Optimal strategy of vaccination $u^*(t)$.

second is to design an optimal vaccination strategy to minimize the number of COVID-19 infections by reformulating the SIR model in Eq. (2.1) by imposing a control variable that represents the effect of the vaccine. Also, we will take into consideration the number of days, $\tau = 14$ days, that the vaccine will start working actively. Then the minimum principle of Pontryagin is implemented to find the optimal vaccination strategy and prevent its spread in Iraq. For this purpose, the results show the impact of the vaccination process on controlling and preventing the spread of COVID-19 in Iraq.

To make this analysis more reliable, we used the data from January 1, 2021, as the initial values. Also, to predict the behavior of the COVID-19 pandemic in Iraq, we documented and drew some figures, see Figs. 4–6. Indeed, the blue curve in these figures clarifies the number of susceptible, infected, and recovered individuals, which agree with the total number of recovered individuals until 15 May 2022, when it is 2299985. The red curve in Figs. 4–6 shows that if the vaccination process depicted in Fig. 7 is followed, the number of susceptible, infected individuals will decrease while the cumulative number of recovered individuals will increase. Many changes can be made to improve this optimal vaccination strategy, such as selecting the balancing cost factors D_1 and D_2 based on the requirements of the Iraqi Ministry of Health or any other beneficiary. In addition, we can account for the effectiveness of any vaccine by assuming the new control variable, $u(t) = \rho v(t)$, where ρ is the vaccine efficacy. In this simulation, $D_1 = 0.001$ and $D_2 = 100$ are used. Also, we assume that the vaccine efficacy is 100%. We hope that this paper will assist the Iraqi Ministry of Health in predicting and controlling the COVID-19 pandemic. In this case, the number of infected people would decrease, as depicted in Fig. 6, while the number of vaccinated and recovered people would increase, as depicted in Fig. 5.

Declaration of competing interest

Data availability

No data was used for the research described in the article.

Acknowledgments

Appendix

Confirmed Coronavirus Cases in Iraq							
Day	Recovery	Infection	Death	*Day*	Recovery	Infection	Death
1/1/2021	1976	902	11	1/2/2021	1929	840	5
1/3/2021	1974	741	5	1/4/2021	1809	595	10
1/5/2021	1928	757	12	1/6/2021	1889	839	9
1/7/2021	1781	790	4	1/8/2021	1898	669	8
1/9/2021	1965	907	4	1/10/2021	1752	607	14
1/11/2021	2035	801	11	1/12/2021	1806	810	5
1/13/2021	1992	867	4	1/14/2021	1784	770	7
1/15/2021	1530	805	10	1/16/2021	2009	596	3
1/17/2021	1531	645	9	1/18/2021	1769	797	9
1/19/2021	1813	823	9	1/20/2021	1909	746	6
1/21/2021	1805	809	9	1/22/2021	1567	685	7
1/23/2021	1546	778	4	1/24/2021	1704	893	5
1/25/2021	1585	813	7	1/26/2021	1625	804	10
1/27/2021	1575	879	8	1/28/2021	1933	943	6
1/29/2021	1280	945	12	1/30/2021	1317	775	5
1/31/2021	1272	714	6	2/1/2021	1255	984	10
2/2/2021	1210	1135	11	2/3/2021	1275	1317	11
2/4/2021	1090	1150	12	2/5/2021	1188	1534	12
2/6/2021	1020	1660	8	2/7/2021	1026	1134	9
2/8/2021	848	1713	6	2/9/2021	977	1994	8
2/10/2021	802	2282	6	2/11/2021	994	2369	4
2/12/2021	1008	2530	13	2/13/2021	1158	2190	7
2/14/2021	1079	2224	15	2/15/2021	1119	2798	6
2/16/2021	1622	3332	7	2/17/2021	1236	3575	12
2/18/2021	1691	3896	16	2/19/2021	1802	4024	12
2/20/2021	1978	3273	13	2/21/2021	2002	3187	27
2/22/2021	2236	3864	23	2/23/2021	2592	4181	16
2/24/2021	2110	4306	13	2/25/2021	2271	4074	27
2/26/2021	2460	4336	14	2/27/2021	2820	3543	18
2/28/2021	2933	3248	23	3/1/2021	3708	3599	22
3/2/2021	3517	4690	30	3/3/2021	3463	5173	25
3/4/2021	3396	5043	24	3/5/2021	3134	5127	30
3/6/2021	3883	4068	11	0 7-03-21	3509	3359	24
3/8/2021	3920	4468	24	3/9/2021	3692	4610	22
3/10/2021	3135	4846	27	3/11/2021	3057	5170	26
3/12/2021	3397	4622	25	3/13/2021	4086	4054	23
3/14/2021	3942	3866	32	3/15/2021	4850	4901	37
3/16/2021	4564	5267	39	3/17/2021	3591	5663	33
3/18/2021	3892	5443	36	3/19/2021	4237	5258	41
3/20/2021	3795	4674	32	8/21/2021	4373	4502	38
8/22/2021	4088	4655	29	8/23/2021	4125	4494	30
8/24/2021	4185	6051	29	8/25/2021	4781	6513	33
8/26/2021	4495	6490	29	8/27/2021	4368	5062	20
8/28/2021	4820	5271	35	8/29/2021	4500	5837	37
8/30/2021	4915	5995	37	8/31/2021	4210	6664	37
4/1/2021	4536	6015	37	4/2/2021	4119	5882	30
4/3/2021	5017	5379	40	4/4/2021	5303	5368	33
4/5/2021	5664	6423	39	4/6/2021	5225	7300	33
4/7/2021	5020	8331	37	4/8/2021	4883	7817	34
4/9/2021	5445	7937	35	4/10/2021	4891	6779	37
4/11/2021	5190	6791	35	4/12/2021	5679	7953	44
4/13/2021	5791	8179	39	4/14/2021	5196	7972	40
4/15/2021	5817	7810	49	4/16/2021	6515	7561	30

Confirmed Coronavirus Cases in Iraq							
Day	Recovery	Infection	Death	*Day*	Recovery	Infection	Death
4/17/2021	5867	6552	33	4/18/2021	6814	6188	33
4/19/2021	7507	7775	45	4/20/2021	6888	8208	36
4/21/2021	6382	8696	38	4/22/2021	6872	8450	30
4/23/2021	6826	8017	46	4/24/2021	6959	6967	43
4/25/2021	7335	6034	40	4/26/2021	7910	6536	46
4/27/2021	7312	7152	45	4/28/2021	7052	6858	44
4/29/2021	7360	6926	41	4/30/2021	7111	6405	32
5/1/2021	7295	5167	33	5/2/2021	7859	4564	38
5/3/2021	7351	5068	30	5/4/2021	7242	6143	42
5/5/2021	7248	5813	32	5/6/2021	7093	6233	33
5/7/2021	6289	5763	29	5/8/2021	6203	4608	39
5/9/2021	6743	4167	30	5/10/2021	6237	4902	29
5/11/2021	6561	5287	34	5/12/2021	5417	4666	21
5/13/2021	5043	4512	28	4/14/2021	5769	2767	27
5/15/2021	5220	2456	24	5/16/2021	5624	2456	24
5/17/2021	5447	3552	41	5/18/2021	6198	4023	34
5/19/2021	5090	4609	40	5/20/2021	5412	4580	33
5/21/2021	4639	4357	35	5/22/2021	4778	3655	21
5/23/2021	5039	3791	32	5/24/2021	4769	4102	24
5/25/2021	4279	4938	27	5/26/2021	3249	4718	26
5/27/2021	4059	4611	22	5/28/2021	3477	4042	22
5/29/2021	5425	3257	23	5/30/2021	4365	3474	17
5/31/2021	4990	4270	24	6/1/2021	4343	4170	30
6/2/2021	4331	4583	31	6/3/2021	4111	4262	26
6/4/2021	4126	4157	26	6/5/2021	4348	3154	30
6/6/2021	4398	3314	20	6/7/2021	4652	4129	28
6/8/2021	4770	4119	23	6/9/2021	4372	4616	25
6/10/2021	4086	4684	34	6/11/2021	4130	4320	20
6/12/2021	4095	3831	22	6/13/2021	4029	3952	15
6/14/2021	4349	5040	31	6/15/2021	4137	4618	26
6/16/2021	3779	5139	19	6/17/2021	3930	5189	30
6/18/2021	3863	5068	23	6/19/2021	3829	3608	26
6/20/2021	3989	4160	25	6/21/2021	4774	5235	25
6/22/2021	5039	6003	25	6/23/2021	4034	6297	33
6/24/2021	4030	6093	31	6/25/2021	4512	5325	34
6/26/2021	4465	4814	28	6/27/2021	4266	4468	30
6/28/2021	4698	6346	30	6/29/2021	5055	6558	35
6/30/2021	4550	7300	30	7/1/2021	4593	7554	30
7/2/2021	5082	6378	40	7/3/2021	5094	5375	25
7/4/2021	5158	6264	35	7/5/2021	5789	8030	29
7/6/2021	5998	8818	31	7/7/2021	5522	8777	37
7/22/2021	7257	8106	81	7/23/2021	8205	8905	66
7/24/2021	8001	7653	65	7/25/2021	8492	9147	55
7/26/2021	9966	12180	60	7/27/2021	8547	12185	71
7/28/2021	8217	23515	66	7/29/2021	9401	13259	49
7/30/2021	8499	12597	62	7/31/2021	8614	10215	62
8/1/2021	7820	9394	77	8/2/2021	8734	12734	68
8/3/2021	7359	11644	63	8/4/2021	6574	12713	73
8/5/2021	7461	11871	62	8/6/2021	8667	11435	87
8/7/2021	9112	7973	59	8/8/2021	9053	8346	57
8/9/2021	8687	9619	67	8/10/2021	9926	9970	66
8/11/2021	9189	8635	66	8/12/2021	9848	10243	64
8/13/2021	9890	9967	75	8/14/2021	10078	7610	65
8/15/2021	9379	7011	66	8/16/2021	9246	8830	68

Confirmed Coronavirus Cases in Iraq						
Day	Recovery	Infection	Death	*Day*	Recovery	Infection	Death
7/8/2021	5139	9189	31	7/9/2021	6508	8636	32
7/10/2021	6106	6821	39	7/11/2021	5937	7616	33
7/12/2021	7098	9149	44	7/13/2021	6708	9046	38
7/14/2021	5813	9635	47	7/15/2021	6505	9337	30
7/16/2021	7805	8336	44	7/17/2021	7920	8149	38
7/18/2021	7964	8698	41	7/19/2021	8278	9883	62
7/20/2021	7613	8922	59	7/21/2021	6916	8320	69
8/17/2021	10477	8778	75	8/18/2021	8113	7992	71
8/19/2021	8760	8012	72	8/20/2021	9224	6121	67
8/21/2021	7651	3958	85	8/22/2021	9647	5634	74
8/23/2021	9142	7151	78	8/24/2021	10242	7670	75
8/25/2021	7961	7787	73	8/26/2021	8728	8084	70
8/27/2021	8011	7202	79	8/28/2021	8153	5369	73
8/29/2021	8152	6083	67	8/30/2021	8193	6778	65
8/31/2021	7148	6937	66	9/1/2021	6595	7309	48
9/2/2021	7265	6948	56	9/3/2021	7828	5672	60
9/4/2021	7415	4316	48	9/5/2021	7706	4897	58
9/6/2021	7480	5650	62	9/7/2021	7517	5988	58
9/8/2021	7046	5405	62	9/9/2021	7644	5073	51
9/10/2021	7298	4717	61	9/11/2021	6685	3086	51
9/12/2021	6789	3554	51	9/13/2021	6702	4204	54
9/14/2021	5802	4400	46	9/15/2021	5725	3895	35
9/16/2021	5763	3923	52	9/17/2021	6633	3559	56
9/18/2021	5082	1959	36	9/19/2021	5067	2515	47
9/20/2021	4878	3192	47	9/21/2021	4454	3081	42
9/22/2021	4989	2906	38	9/23/2021	5335	2953	44
9/24/2021	4507	2964	46	9/25/2021	5310	1312	33
9/26/2021	3658	2139	38	9/27/2021	4156	2447	32
9/28/2021	3795	2401	45	9/29/2021	3389	2254	34
9/30/2021	3497	2434	39	10/1/2021	4395	2688	42
10/2/2021	3803	1236	42	10/3/2021	3363	2451	21
10/4/2021	3184	1956	27	10/5/2021	3243	2470	28
10/6/2021	3225	2519	20	10/7/2021	3150	2044	33
10/8/2021	3251	2215	36	10/9/2021	3313	1227	28
10/10/2021	3531	1652	26	10/11/2021	3205	944	28
10/12/2021	3472	1644	29	10/13/2021	3245	1766	35
10/14/2021	3179	2383	26	10/15/2021	3199	2162	32
10/16/2021	3007	1077	25	10/17/2021	3189	1716	18
10/18/2021	2851	1559	29	10/19/2021	3256	1835	25
10/20/2021	2938	1388	26	10/21/2021	2656	1882	39
10/22/2021	2669	1846	26	10/23/2021	2207	1064	36
10/24/2021	2139	1247	24	10/25/2021	2588	1537	32
10/26/2021	2409	1429	31	10/27/2021	2302	1412	37
10/28/2021	2249	1471	22	10/29/2021	2433	1397	28
10/30/2021	1952	682	27	10/31/2021	1861	1046	32
11/1/2021	1973	1153	26	11/2/2021	1925	1315	27
11/3/2021	1812	1198	25	11/4/2021	1839	1152	23
11/5/2021	1871	1156	26	11/6/2021	1665	717	22
11/7/2021	1405	924	25	11/8/2021	1437	1148	28
11/9/2021	1524	1116	27	11/10/2021	1621	915	16
11/11/2021	1412	863	30	11/12/2021	1452	892	26
11/13/2021	1375	591	12	11/14/2021	1374	859	20
11/15/2021	1330	829	33	11/16/2021	1173	807	26
11/17/2021	1181	806	18	11/18/2021	1347	789	27
11/19/2021	1216	789	21	11/20/2021	1006	568	14
11/21/2021	705	584	23	11/22/2021	1281	829	21

Confirmed Coronavirus Cases in Iraq

Day	Recovery	Infection	Death	Day	Recovery	Infection	Death
11/23/2021	1334	898	26	11/24/2021	1377	776	13
11/25/2021	1182	743	23	11/26/2021	1423	856	17
11/27/2021	1366	563	7	11/28/2021	1321	538	21
11/29/2021	1367	826	14	11/30/2021	1355	724	13
12/1/2021	1203	889	24	12/2/2021	1042	713	15
12/3/2021	1112	741	8	12/4/2021	816	374	6
12/5/2021	839	457	12	12/6/2021	927	615	18
12/7/2021	952	625	16	12/8/2021	744	606	12
12/9/2021	762	510	12	12/10/2021	663	545	16
12/11/2021	615	250	6	12/12/2021	758	340	13
12/13/2021	783	522	16	12/14/2021	696	474	13
12/15/2021	573	462	10	12/16/2021	800	410	13
12/17/2021	688	357	12	12/18/2021	480	182	9
12/19/2021	392	272	12	12/20/2021	547	364	11
12/21/2021	456	336	13	12/22/2021	490	342	8
12/23/2021	422	312	13	12/24/2021	466	322	7
12/25/2021	401	156	7	12/26/2021	335	172	8
12/27/2021	435	166	9	12/28/2021	390	225	7
12/29/2021	363	261	5	12/30/2021	356	300	3
12/31/2021	443	304	4	1/1/2022	238	151	5
1/2/2022	226	206	4	1/3/2022	289	252	7
1/4/2022	326	318	8	1/5/2022	320	516	9
1/6/2022	344	665	3	1/7/2022	241	642	4
1/8/2022	180	316	2	1/9/2022	248	734	7
1/10/2022	310	1368	5	1/11/2022	384	1610	8
1/12/2022	281	2037	5	1/13/2022	370	2385	4
1/14/2022	397	3266	8	1/15/2022	335	2477	5
1/16/2022	431	3630	5	1/17/2022	582	4466	5
1/18/2022	648	6487	10	1/19/2022	718	6234	5
1/20/2022	885	5767	5	1/21/2022	1995	7155	5
1/22/2022	1704	4884	6	1/23/2022	2000	4931	4
1/24/2022	2756	5756	13	1/25/2022	3025	7693	9
1/26/2022	3154	8107	10	1/27/2022	3458	7609	11
1/28/2022	4559	8554	17	1/29/2022	3962	5827	14
1/30/2022	5657	5582	15	1/31/2022	5759	7217	13
2/1/2022	6550	7910	16	2/2/2022	6333	8293	25
2/3/2022	6253	6949	25	2/4/2022	7312	6569	21
2/5/2022	4922	4316	23	2/6/2022	5259	3589	17
2/7/2022	6881	5285	27	2/8/2022	7100	5360	27
2/9/2022	6000	4681	30	2/10/2022	5504	4220	26
2/11/2022	5718	3776	29	2/12/2022	4323	2014	23
2/13/2022	5228	2036	26	2/14/2022	6171	3011	25
2/15/2022	5938	2984	35	2/16/2022	4570	2639	28
2/17/2022	3849	2246	32	2/18/2022	4434	2326	16
2/19/2022	3668	1234	11	2/20/2022	3940	1159	7
2/21/2022	3815	2074	18	2/22/2022	3477	1685	21
2/23/2022	2963	1736	20	2/24/2022	2606	1499	14
2/25/2022	2659	1603	17	2/26/2022	2232	878	12
2/27/2022	2544	945	15	2/28/2022	2643	1203	14
3/1/2022	2829	1023	10	3/2/2022	2343	1267	14
3/3/2022	2088	1009	15	3/4/2022	1916	1066	6
3/5/2022	1346	397	7	3/6/2022	1536	636	9
3/7/2022	1806	737	18	3/8/2022	1560	888	8
3/9/2022	1765	723	6	3/10/2022	1289	699	8

Confirmed Coronavirus Cases in Iraq

Day	Recovery	Infection	Death	Day	Recovery	Infection	Death
3/11/2022	1563	688	4	3/12/2022	1123	366	3
3/13/2022	1326	421	2	3/14/2022	1289	657	6
3/15/2022	1346	573	4	3/16/2022	1012	632	7
3/17/2022	1028	559	3	3/18/2022	988	439	5
3/19/2022	666	218	3	3/20/2022	945	253	2
3/21/2022	957	262	2	3/22/2022	984	187	1
3/23/2022	770	265	2	3/24/2022	1006	370	4
3/25/2022	746	370	7	3/26/2022	855	249	4
3/27/2022	883	230	1	3/28/2022	815	743	6
3/29/2022	728	415	4	3/30/2022	537	344	3
3/31/2022	578	341	1				

References

[1] Craig AM, Hughes BL, Swamy GK. Coronavirus disease 2019 vaccines in pregnancy. Amer J Obstetrics Gynecol MFM 2021;3(2):100295. http://dx.doi.org/10.1016/j.ajogmf.2020.100295.
[2] Anderson RM, May RM. Population biology of infectious diseases: Part I. Nature 1979;280(5721):361–7. http://dx.doi.org/10.1038/280361a0.
[3] Anderson RM, Lee PA. Infectious diseases of humans. OUP Oxford; 1992, URL https://www.ebook.de/de/product/3246618/roy_m_anderson_pamela_anderson_lee_infectious_diseases_of_humans.html.
[4] Diekmann O, Heesterbeek J. Mathematical epidemiology of infectious diseases: Model building, analysis and interpretation. Wiley series in mathematical and computational biology, United States: John Wiley and Sons; 2000.
[5] Kucharski AJ, Russell TW, Diamond C, Liu Y, Edmunds J, Funk S, et al. Early dynamics of transmission and control of COVID-19: A mathematical modelling study. Lancet Infect Dis 2020;20(5):553–8.
[6] Liu Y, Gayle AA, Wilder-Smith A, Rocklöv J. The reproductive number of COVID-19 is higher compared to SARS coronavirus. J Travel Med 2020;27(2). http://dx.doi.org/10.1093/jtm/taaa021.
[7] Ivorra B, Ferrández M, Vela-Pérez M, Ramos A. Mathematical modeling of the spread of the coronavirus disease 2019 (COVID-19) taking into account the undetected infections. The case of China. Commun Nonlinear Sci Numer Simul 2020;88:105303. http://dx.doi.org/10.1016/j.cnsns.2020.105303.
[8] Tuan NH, Mohammadi H, Rezapour S. A mathematical model for COVID-19 transmission by using the Caputo fractional derivative. Chaos Solitons Fractals 2020;140:110107. http://dx.doi.org/10.1016/j.chaos.2020.110107.
[9] Al-Saedi HM, Hameed HH. Mathematical modeling for COVID-19 pandemic in Iraq. J Interdiscipl Math 2021;24(5):1407–27. http://dx.doi.org/10.1080/09720502.2021.1923943.
[10] Lenhart S, Workman JT. Optimal control applied to biological models. Chapman and Hall/CRC; 2007.
[11] Asamoah JKK, Okyere E, Abidemi A, Moore SE, Sun G-Q, Jin Z, et al. Optimal control and comprehensive cost-effectiveness analysis for COVID-19. Results Phys 2022;33:105177. http://dx.doi.org/10.1016/j.rinp.2022.105177.
[12] Asamoah JKK, Bornaa C, Seidu B, Jin Z. Mathematical analysis of the effects of controls on transmission dynamics of SARS-CoV-2. Alex Eng J 2020;59(6):5069–78. http://dx.doi.org/10.1016/j.aej.2020.09.033.
[13] Asamoah JKK, Jin Z, Sun G-Q. Non-seasonal and seasonal relapse model for Q fever disease with comprehensive cost-effectiveness analysis. Results Phys 2021;22:103889. http://dx.doi.org/10.1016/j.rinp.2021.103889.
[14] Faniran TS, Ali A, Al-Hazmi NE, Asamoah JKK, Nofal TA, Adewole MO. New variant of SARS-CoV-2 dynamics with imperfect vaccine. In: Selişteanu D, editor. Complexity 2022;2022:1–17. http://dx.doi.org/10.1155/2022/1062180.
[15] Khalaf SL, Kadhim MS, Khudair AR. Studying of COVID-19 fractional model: Stability analysis. Part Diff Equ Appl Math 2023;7:100470. http://dx.doi.org/10.1016/j.padiff.2022.100470.
[16] Wu J, Tang B, Bragazzi NL, Nah K, McCarthy Z. Quantifying the role of social distancing, personal protection and case detection in mitigating COVID-19 outbreak in Ontario, Canada. J Math Ind 2020;10(1). http://dx.doi.org/10.1186/s13362-020-00083-3.
[17] Fanelli D, Piazza F. Analysis and forecast of COVID-19 spreading in China, Italy and France. Chaos Solitons Fractals 2020;134:109761. http://dx.doi.org/10.1016/j.chaos.2020.109761.
[18] Atangana A. Modelling the spread of COVID-19 with new fractal-fractional operators: Can the lockdown save mankind before vaccination? Chaos Solitons Fractals 2020;136:109860. http://dx.doi.org/10.1016/j.chaos.2020.109860.
[19] Şahin U, Şahin T. Forecasting the cumulative number of confirmed cases of COVID-19 in Italy, UK and USA using fractional nonlinear grey Bernoulli model. Chaos Solitons Fractals 2020;138:109948. http://dx.doi.org/10.1016/j.chaos.2020.109948.
[20] Torrealba-Rodriguez O, Conde-Gutiérrez R, Hernández-Javier A. Modeling and prediction of COVID-19 in Mexico applying mathematical and computational models. Chaos Solitons Fractals 2020;138:109946. http://dx.doi.org/10.1016/j.chaos.2020.109946.
[21] Asamoah JKK, Owusu MA, Jin Z, Oduro F, Abidemi A, Gyasi EO. Global stability and cost-effectiveness analysis of COVID-19 considering the impact of the environment: Using data from Ghana. Chaos Solitons Fractals 2020;140:110103. http://dx.doi.org/10.1016/j.chaos.2020.110103.
[22] Asamoah JKK, Jin Z, Sun G-Q, Seidu B, Yankson E, Abidemi A, et al. Sensitivity assessment and optimal economic evaluation of a new COVID-19 compartmental epidemic model with control interventions. Chaos Solitons Fractals 2021;146:110885. http://dx.doi.org/10.1016/j.chaos.2021.110885.
[23] Acheampong E, Okyere E, Iddi S, Bonney JH, Asamoah JKK, Wattis JA, et al. Mathematical modelling of earlier stages of COVID-19 transmission dynamics in Ghana. Results Phys 2022;34:105193. http://dx.doi.org/10.1016/j.rinp.2022.105193.
[24] Moore SE, Nyandjo-Bamen HL, Menoukeu-Pamen O, Asamoah JKK, Jin Z. Global stability dynamics and sensitivity assessment of COVID-19 with timely-delayed diagnosis in Ghana. Comput Math Biophys 2022;10(1):87–104. http://dx.doi.org/10.1515/cmb-2022-0134.
[25] Ngonghala CN, Iboi E, Eikenberry S, Scotch M, MacIntyre CR, Bonds MH, et al. Mathematical assessment of the impact of non-pharmaceutical interventions on curtailing the 2019 novel coronavirus. Math Biosci 2020;325:108364. http://dx.doi.org/10.1016/j.mbs.2020.108364.
[26] Addai E, Zhang L, Asamoah JKK, Preko AK, Arthur YD. Fractal–fractional age-structure study of Omicron SARS-CoV-2 variant transmission dynamics. Partial Differ Equ Appl Math 2022;6:100455. http://dx.doi.org/10.1016/j.padiff.2022.100455.
[27] Addai E, Zhang L, Preko AK, Asamoah JKK. Fractional order epidemiological model of SARS-CoV-2 dynamism involving Alzheimer's disease. Healthc Anal 2022;2:100114. http://dx.doi.org/10.1016/j.health.2022.100114.

[28] Khudair AR. On solving non-homogeneous fractional differential equations of Euler type. Comput Appl Math 2013;32(3):577–84. http://dx.doi.org/10.1007/s40314-013-0046-2.

[29] Khudair AR, Haddad S, khalaf SL. Restricted fractional differential transform for solving irrational order fractional differential equations. Chaos Solitons Fractals 2017;101:81–5. http://dx.doi.org/10.1016/j.chaos.2017.05.026.

[30] Khalaf SL, Khudair AR. Particular solution of linear sequential fractional differential equation with constant coefficients by inverse fractional differential operators. Differ Equ Dyn Syst 2017;25(3):373–83. http://dx.doi.org/10.1007/s12591-017-0364-8.

[31] Jalil AFA, Khudair AR. Toward solving fractional differential equations via solving ordinary differential equations. Comput Appl Math 2022;41(1). http://dx.doi.org/10.1007/s40314-021-01744-8.

[32] Iraq Population (1950 - 2020). https://www.worldometers.info/world-population/iraq-population/.

[33] van den Driessche P, Watmough J. Reproduction numbers and sub-threshold endemic equilibria for compartmental models of disease transmission. Math Biosci 2002;180(1–2):29–48.

[34] Chitnis N, Hyman JM, Cushing JM. Determining important parameters in the spread of malaria through the sensitivity analysis of a mathematical model. Bull Math Biol 2008;70(5):1272–96. http://dx.doi.org/10.1007/s11538-008-9299-0.

[35] Göllmann L, Kern D, Maurer H. Optimal control problems with delays in state and control variables subject to mixed control-state constraints. Optim Control Appl Methods 2009;30(4):341–65. http://dx.doi.org/10.1002/oca.843.